

# Variable Impedance Actuator with Exponential Elasticity for Flexible-Joint-Robot and Estimation of the Joint Impedance

Soumen Sen, and Chandan Har  
Robotics & Automation Division  
CSIR - Central Mechanical Engineering Research Institute  
Durgapur, INDIA  
soumen\_sen@cmcri.res.in, and har\_chandan@yahoo.co.in

Sananda Chatterjee  
Bengal Engineering and Science University, Shibpur and  
CSIR - CMERI Mechatronics Programme  
Durgapur, INDIA  
sanandachatterjee@ymail.com

**Abstract**—New generation robots, meant for physical human robot interactions, are no longer rigid; it has become soft in terms of introduction of considerable flexibility at the actuated joints, flexibility of the links and in terms of compliant coverings. Safety requirement becomes primary in situations where physical interactions occur, calling for compliance; but accuracy and control bandwidth get compromised. While it has been established in literature that flexible-link-robots are difficult to control, it is found feasible to recover some of the lost bandwidth by varying stiffness in flexible-joint-robots, maintaining safety of human during interaction. This article addresses development of such a flexible robot joint actuation system with stiffness/impedance variability. This variability of stiffness is achieved passively by the flexible transmission interposed between the prime mover and the actuated link, and in doing so, *nonlinearity* in the elastic transmission characteristic becomes essential. The Variable Stiffness Actuation (VSA) system of this article employs an elastic element having an exponential force-displacement characteristic, which has the property of stiffness varying linearly with transmission force. This property is favourably utilized in the estimation of stiffness, and in turn can be used in control of stiffness. The variable stiffness actuation is realized here by assembling two transmissions in agonist-antagonistic arrangement in order to achieve simultaneous control of both joint-motion and stiffness, resembling biological musculo-skeletal system. By adding nonlinear damping elements in parallel to the elastic transmission, variability in mechanical impedance has been achieved. Joint stiffness is computed with the estimated stiffness of individual transmissions, which are obtained experimentally. Extended Kalman Filter is employed for the estimation of stiffness and other impedance components. Results are reported in support of the effectiveness of the joint actuator in achieving variability in stiffness and impedance and their estimation.

**Keywords** – *Exponential elastic transmission; Mechanical impedance; Variable-Stiffness/Impedance-Actuation; Agonist-Antagonistic arrangement; Extended Kalman Filter*

## I. INTRODUCTION

Introduction of flexibility and variation of intrinsic passive impedance is becoming essential in enhancing ability

and performance of actuation systems in safety critical applications involving physical-human-machine-interaction, in many cases the machine being a robot. Unlike conventionally actuated machine joints, here the joints are not rigid. This implies that there exists a flexibility in the transmission between the actuator shaft and the actuated joint shaft. In variable stiffness/impedance actuation, this joint compliance varies according to the need of task execution. In physically interactive tasks by machine with operators, the safety of human is of prime importance. A joint can be made safe against accidental impact hazards of fast moving machine parts by attenuating the reflected inertia through the compliance (see [1]). Hazard due to impact is a function of effective inertia and relative velocity of the impacting body. Thus, during a task execution, when positional accuracy is more demanding, the joint can be made stiff at low velocity, where as during gross motion with high velocity, the joint can be made compliant, maintaining operator's safety intrinsically against accidental impact. This requirement leads to variability in stiffness and in turn impedance.

Impedance control, as a general method, has been put through for robotic manipulation in interactive tasks by Neville Hogan with the seminal work in [2]. However, as early as in 1977, probably the first ever programmable stiffness control device was built by Hanafusa and Asada ([3]) in a mechanical hand. Nevertheless, impedance variability in everyday task ever prevail in the biological world (e.g. [4]). Variable stiffness mechanisms have been successfully implemented in other fields of research as well, such as legged locomotion, exoskeletons and rehabilitation devices, in structural vibration control, and automotive suspension system. One important attribute of stiffness variability here is that it is achieved *passively*, and not by active control. A passively variable stiffness mechanism possesses an elastic element or *spring*, where the transmitted force bears a *nonlinear* relationship with the deflection of the element undergoes. Many of the designs of elastic transmissions in literature have been done not considering a specified elastic function in the first place. In such designs either a nonlinear

elastically deformable material (e.g. rubber) has been used, or, a mechanism with a *linear* spring has been built ([5], [6], [7], [8]). This article presents development of a new variable stiffness/impedance joint actuator, where, the elastic function of the transmission is designed from a first principle obtained from passive property of biological muscle. Subsequently, the report presents a method for joint impedance estimation.

## II. DESIGN OF NONLINEAR ELASTIC TRANSMISSION ELEMENT

In obtaining variability in stiffness passively, the elastic element should essentially possess a nonlinear *force-displacement* characteristic. The design of elastic element gets motivated from the nonlinear passive elastic behaviour of an animal muscle fibre.

### A. Principle

The principle is obtained from a mathematical model of biological muscle fibre from literature. Muscle fibres are found to become progressively stiffer on stretching passively. Pinto and Fung ([9]) observed experimentally (on rabbit heart muscle) that derivative of muscle *stress*,  $s$  with respect to *Lagrangian strain*,  $\epsilon_L$  is proportional to stress  $s$  at that point. This leads to

$$\frac{L_0}{A} \frac{dF_S}{dx} = \alpha \left( \frac{F_S}{A} + \beta \right), \quad (1)$$

where,  $F_S \geq 0$  is the force transmitted,  $A$  the constant cross sectional area,  $x \geq 0$  is the elongation,  $L_0 =$  rest length, and  $\alpha$  and  $\beta$  are constants. This passive behaviour of a muscle fibre gives rise to an interesting property, where, the stiffness of the elastic transmission becomes linearly related to the transmitted force and the force displacement function thus bears an *exponential* characteristic (see author's paper [10] for derivation). Defining stiffness as  $\sigma = \frac{\partial F_\sigma}{\partial x}$ , force function and stiffness are given by the following:

$$F_S = \Phi(x) = F_0 + F_\sigma = F_0 + k_1 \exp(k_2 x), \quad (2)$$

where  $F_0$  is an initial force offset,  $F_\sigma$  is the elastic force.  $k_1$  and  $k_2$  are constant coefficients and they can be estimated using  $L_0$ ,  $A$ ,  $\alpha$  and  $\beta$  in (1). This leads to linearity between stiffness  $\sigma$  and  $F_\sigma$ ,

$$\sigma = k_2 F_\sigma. \quad (3)$$

The linear property is favourably used in the estimation of impedance parameters through an EKF procedure.

### B. Spring Design and Physical Realization

In order to obtain the elastic function of (2), first a specification set is needed in terms of (i) maximum elastic deflection  $X_{max}$ , (ii) maximum force to be transmitted  $F_{Smax}$ , (iii) minimum force, or force bias  $F_{Smin}$ , (iv) rest length/preloading  $L_0$ , (v) smallest deflection  $\delta_0$  and relative force error at  $x = 0$ ,  $C_0$ . The relative force error is defined as  $\frac{\delta F_S}{F_S} = \frac{1}{\Phi(x)} \frac{d\Phi(x)}{dx} \delta x$ . The detailed procedure for designing the spring can be found in [10].

For the chosen specification of maximum load capacity  $F_{Smax} = 200N$ , maximum deformation  $X_{max} = 20mm$ ,  $L_0 = 5mm$ ,  $F_{Smin} = 5N$ ,  $C_0 = 0.2N/N$  and  $\delta_0 = 1mm$ , value of  $k_2$  is found to be 0.2658 ( $\alpha = 1.3288$ ). The desired spring function thus derived to be

$$F_S = 0.9772 \exp(0.2658x) + 1.2372, \quad x \geq 0. \quad (4)$$

It is to be noted that the stiffness does not depend on the force offset  $F_0$ . In practice, the force bias will show a different value and will depend on the size of the physical step in the beginning of the machined profile (see middle and right figures of Fig. 1).

The physical realization of the exponential function is achieved through using a cam surface and spring loaded cam-follower mechanism. The cam profile is synthesized in such a way that the pulling force on the pulling rod of the spring follows the exponential function. Principle for profile synthesis is shown in left figure of Fig. 1, while the middle figure shows the actual profile surface. The cam profile is realized in an aluminium block by CNC milling. A V-groove provides guidance to the cam-follower roller, which is again loaded by a linear spring. The design spring constant of the linear springs is  $5N/mm$ ; although the actual linear springs used in the spring assemblies differ in the values of spring rate.

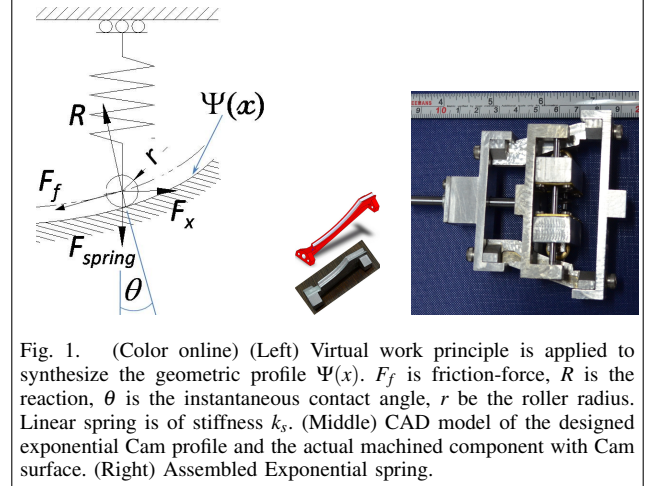


Fig. 1. (Color online) (Left) Virtual work principle is applied to synthesize the geometric profile  $\Psi(x)$ .  $F_f$  is friction-force,  $R$  is the reaction,  $\theta$  is the instantaneous contact angle,  $r$  be the roller radius. Linear spring is of stiffness  $k_s$ . (Middle) CAD model of the designed exponential Cam profile and the actual machined component with Cam surface. (Right) Assembled Exponential spring.

In the present article, an antagonistic joint has been developed with two such springs as nonlinear transmission elements. However, the actual elastic characteristics of both the nonlinear transmissions show deviation from the designed one due to the difference in the spring constants of the linear springs on cam-follower used in the construction, assumption of zero roller radius, and dimensional tolerance of manufactured components. A step in the beginning of the profile surface decides the force offset, which becomes different in different assemblies.

### C. Nonlinear Damped Elastic Transmission

A nonlinear damping element is added in parallel with the elastic element by using an off-the-shelf *miniature damper* obtained from ACE GmBh, model FRT-D2-152. The force velocity characteristic from data sheet is well represented by an odd polynomial function

$$F_d = d_0 \text{sgn}(\dot{x}) + d_1 \dot{x} + d_2 \dot{x}^3, \quad (5)$$

where,  $d_1$  and  $d_2$ , are constant coefficients,  $d_2$  being negative and  $d_0$  is the coulomb friction. The damping element is shown in the photograph and in the solid model of Fig. 2

The rotary damper and a miniature encoder of Hengstler make (model PC9S051204N) are mounted through a rotary-to-linear conversion. A miniature tensile force sensor of make Futek (model *FBB300*) is attached at the pulling rod end to measure the total transmission force. The assembly of the nonlinear transmission is presented in the photograph of Fig. 2.

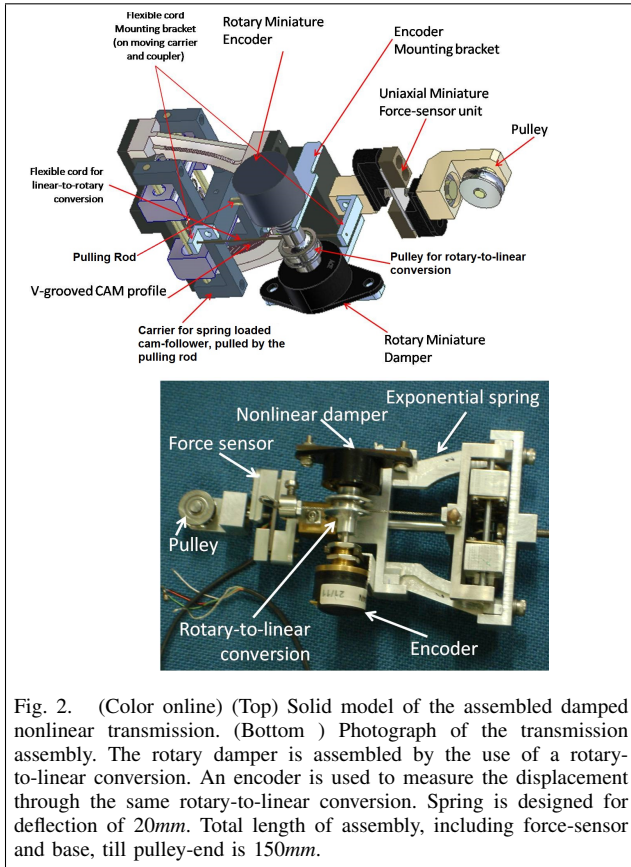


Fig. 2. (Color online) (Top) Solid model of the assembled damped nonlinear transmission. (Bottom) Photograph of the transmission assembly. The rotary damper is assembled by the use of a rotary-to-linear conversion. An encoder is used to measure the displacement through the same rotary-to-linear conversion. Spring is designed for deflection of 20mm. Total length of assembly, including force-sensor and base, till pulley-end is 150mm.

### III. VARIABLE STIFFNESS/IMPEDANCE ACTUATOR

Variable stiffness actuators can be realized broadly in two ways: (1) through explicit stiffness control, where an independent motor is used for stiffness variation, and (2) agonist-antagonistic realization, where, two motors are used in the same time for simultaneous control of motion and

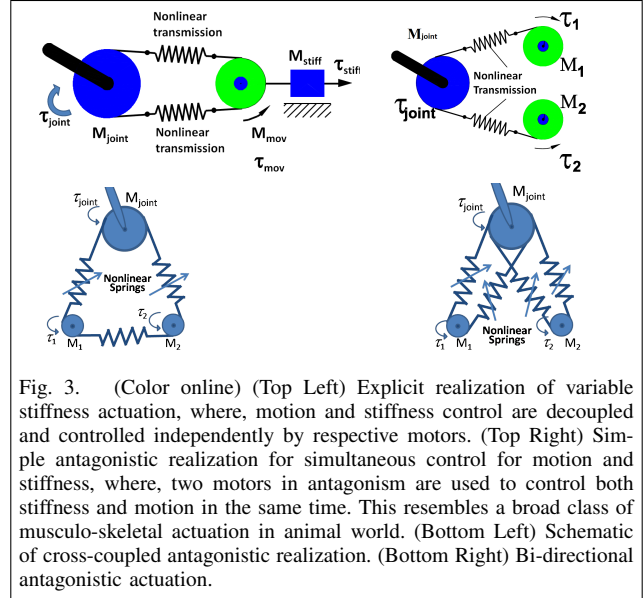


Fig. 3. (Color online) (Top Left) Explicit realization of variable stiffness actuation, where, motion and stiffness control are decoupled and controlled independently by respective motors. (Top Right) Simple antagonistic realization for simultaneous control for motion and stiffness, where, two motors in antagonism are used to control both stiffness and motion in the same time. This resembles a broad class of musculo-skeletal actuation in animal world. (Bottom Left) Schematic of cross-coupled antagonistic realization. (Bottom Right) Bi-directional antagonistic actuation.

stiffness of the joint. These are illustrated in Fig. 3. Again, antagonistic realizations can be broadly divided into (a) simple antagonistic, (b) cross-coupled antagonistic and (c) bi-directional antagonistic arrangements (see [11]). In this article, development of a variable-stiffness-actuator through simple antagonistic realization is reported, which resembles a broad class of biological musculo-skeletal actuation system.

#### A. Development of Simple Antagonistic Actuator

A Variable Impedance Actuator is assembled with the simple antagonistic realization utilizing two damped-elastic-transmissions developed in the previous section. The actuator joint consists of a joint shaft, driven by a capstan pulley, which in turn is actuated by two positive drive tendons. Multi-strand steel wire-ropes are used as tendons. Tendons are pulled by two geared DC motors. In each side of the antagonistic arrangement, the nonlinear transmission element is interposed between the motor pulley and the capstan pulley in series with the tendon. Tendon in each side is routed through idle pulleys in such a way that the force sensed by the force-sensor on the pulling rod (see Fig. 2) is twice the tendon tension. The whole flexible joint assembly is illustrated in the solid model and the photograph of Fig. 4.

### IV. TRANSMISSION AND ACTUATOR MODEL

The transmission is modeled by dynamics of a spring-damper-mass system, with the nonlinear elastic and damping described before:

$$F(t) = F_M(\ddot{x}(t)) + F_d(\dot{x}(t)) + F_\sigma(x(t)) + d_0 \text{sgn}(\dot{x}) + F_0, \quad (6)$$

where,  $F_M = m\ddot{x}$ ,  $F_S = F_\sigma + F_0$ ,  $d_0$  is the static friction, and  $t$  is time. Elastic and Damping force functions are given

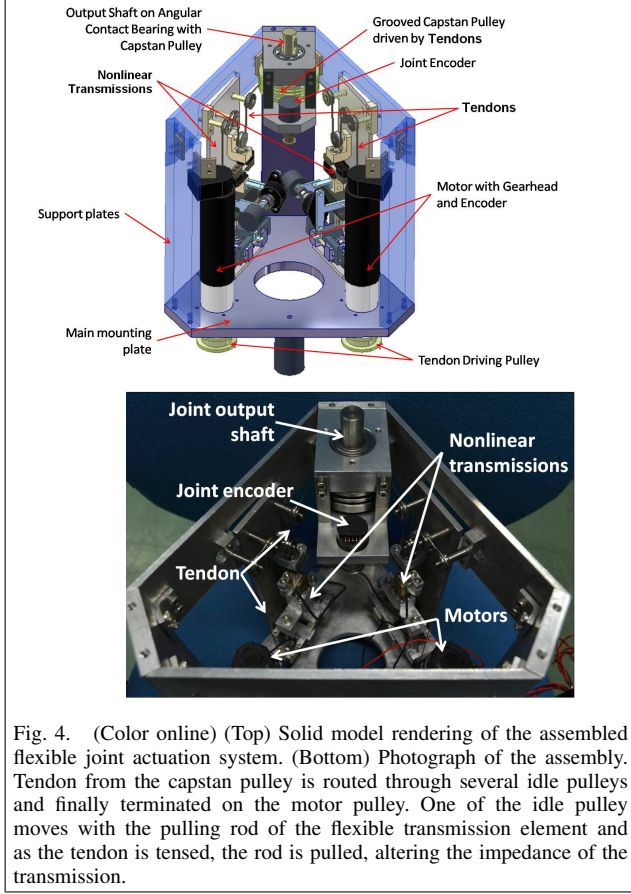


Fig. 4. (Color online) (Top) Solid model rendering of the assembled flexible joint actuation system. (Bottom) Photograph of the assembly. Tendon from the capstan pulley is routed through several idle pulleys and finally terminated on the motor pulley. One of the idle pulley moves with the pulling rod of the flexible transmission element and as the tendon is tensed, the rod is pulled, altering the impedance of the transmission.

by equations (2) and (5) respectively. The implicit dynamic force balance in (6) (in terms of unknown coefficients) can, therefore, be expressed as

$$F = f(x, \dot{x}, \ddot{x}, d_0, d_1, d_2, k_1, k_2, F_0, m) \quad (7)$$

and the problem reduces to identifying the unknown coefficients. To note that,  $k_2$  does not appear linearly in (2), in contrary to other parameters, which appear linearly. This problem is overcome in Extended Kalman Filter by estimating only the *stiffness*, exploiting the *linear* relation between stiffness and force (instead of *full* parameter estimation of the *force-displacement* function).

#### A. Impedance of the Nonlinear Transmission

*Impedance* is said to be the resistance of the transmission manifested in changing the dynamic states of it. Impedance components of the transmission are defined as

$$\begin{aligned} \text{Generalized Stiffness:} \quad & \sigma = \frac{\partial f}{\partial x} \\ \text{Generalized Damping:} \quad & D = \frac{\partial f}{\partial \dot{x}} \\ \text{Generalized Inertia:} \quad & M = \frac{\partial f}{\partial \ddot{x}} \end{aligned} \quad (8)$$

and the following differential form is obtained:

$$\delta F = M\delta\ddot{x} + D\delta\dot{x} + \sigma\delta x. \quad (9)$$

In practice, it is very difficult to directly measure the impedance components by evaluating the ratios of respective differential forces and differential motions, especially, in steady states. A direct method, in principle, requires knowledge of the elastic and damping models in (2) and (5) respectively.

#### B. Stiffness and Impedance at the Joint

In modeling the entire transmission, each tendon is considered as a *linear* spring in series with the nonlinear lumped mass-spring-damper system as shown in Fig. 5.

Let, the stiffness of the joint is set by moving the motors (configured as position actuators), as shown in the figure, such that the system attains an equilibrium configuration and at that operating point the stiffness of the nonlinear spring is set at a value of  $\sigma_{noni}$ ,  $i = 1, 2$ . Once reached an equilibrium, the joint is kept at stationary. The force sensor on each branch measures twice the tendon tension. Similarly, encoder on each nonlinear spring measures half the net displacement the tendon undergoes. Let, the effective stiffness of the *linear* tendon (routed over the pulleys) be  $K_{tendoni}$ ,  $i = 1, 2$ . Net stiffness of each branch then becomes

$$K_{branchi} = \frac{\sigma_{noni} K_{tendoni}}{\sigma_{noni} + 4K_{tendoni}}, \quad i = 1, 2. \quad (10)$$

Let  $R$  denotes the mean radius of the capstan pulley. Then the stiffness at the joint  $K_\theta$  is derived in a straight forward way to be

$$K_\theta = R^2 \sum_{i=1}^2 \frac{\sigma_{noni} K_{tendoni}}{\sigma_{noni} + 4K_{tendoni}} \quad (11)$$

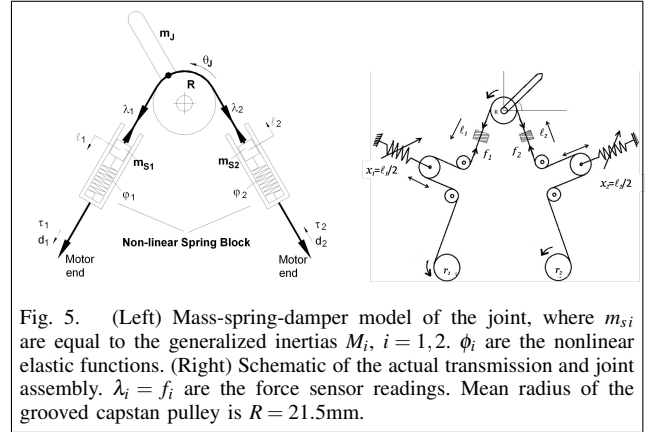


Fig. 5. (Left) Mass-spring-damper model of the joint, where  $m_{si}$  are equal to the generalized inertias  $M_i$ ,  $i = 1, 2$ .  $\phi_i$  are the nonlinear elastic functions. (Right) Schematic of the actual transmission and joint assembly.  $\lambda_i = f_i$  are the force sensor readings. Mean radius of the grooved capstan pulley is  $R = 21.5\text{mm}$ .

If, the inertia of the robot joint shaft (and link) is  $J_{joint}$  and  $m_{s1}$  and  $m_{s2}$  are the lumped masses in the nonlinear transmission model, then the effective robot joint inertia (constant) becomes

$$J_\theta = \frac{1}{2} (M_1 + M_2) R^2 + J_{joint}, \quad (12)$$

where,  $M_i = m_{si}$  are generalized inertia and constant. Similarly, at any operating point (velocity) of the nonlinear

spring units, if the generalized damping rates are  $D_1$  and  $D_2$ , then with the constant damping present at the joint ( $D_{joint}$ ), effective joint damping rate becomes

$$D_{\theta} = \frac{1}{2}(D_1 + D_2)R^2 + D_{joint}. \quad (13)$$

Following section will discuss the estimation of the impedance components of the transmissions ( $\sigma_{noni}$ ,  $D_i$  and  $M_i$ ,  $i = 1, 2$ ) and in turn the estimation for the joint.

## V. ESTIMATION OF IMPEDANCE

Some work on estimation of impedance in variable-impedance-actuation is available in literature; for example, [12] attempts a model free parametric approach, and [13] employs concept of residual torque for model free estimation of impedance in flexible systems. In this article estimation of impedance components in (8) is attempted employing a first order Extended Kalman Filter to estimate dynamic states and parameters of a partial model simultaneously and a procedure is developed. The novelty of the method is that it does NOT utilize the direct force model of (7) (i.e. the elastic model in (2) where  $k_2$  appear nonlinearly) and damping model in (5). The stiffness-force linearity of the exponential elastic function in (3) is exploited to eliminate parameter nonlinearity.

### A. Estimation of Impedance using Stiffness-Force Linearity

This formulation requires knowledge of force rate, so that only  $k_2$  needs to be estimated for generalized stiffness and only  $d_2$  for generalized damping; the force offset,  $F_0$  and coulomb friction  $d_0$  do not either appear in the formulation (since they are independent of the dynamic states). It is assumed that the following derivative exists

$$\dot{F}(t) = \frac{\partial F_S}{\partial x} \dot{x}(t) + \frac{\partial F_d}{\partial \dot{x}} \ddot{x}(t) + \frac{\partial F_M}{\partial \ddot{x}} \ddot{\ddot{x}}(t), \quad (14)$$

such that  $\dot{F} = \sigma \dot{x} + D \ddot{x} + M \ddot{\ddot{x}}$  using definitions in (8).

Time rate of stiffness is given by

$$\dot{\sigma}(t) = k_2 \sigma \dot{x}, \quad (15)$$

and the time derivative of the damping rate is obtained as

$$\dot{D} = 6d_2 \dot{x} \ddot{x}. \quad (16)$$

Equations (14), (15) and (16) are used in the EKF formulation in estimating the states  $x$ ,  $\dot{x}$  and  $\ddot{x}$  and the impedance components  $\sigma(t)$ ,  $D(t)$  and  $M$ . The pretension force  $F_0$  and the static friction  $d_0$  can be estimated in a parallel filter (which may be done at a slower rate) based on the total measured force and the total estimated impedance force.

### B. EKF Implementation

In this *EKF* framework for simultaneous state and impedance estimation, only  $k_2$  and  $d_2$  appear in the state vector. The estimator needs time rate of force as input, which is obtained using a first order filter from the force-sensor data. Measurement in the filter is the deflection; velocity and acceleration are estimated within the filter.

Defining the state vector as  $Z = \{z_i | i = 1 \text{ to } 8\} = [x \ \dot{x} \ \ddot{x} \ \sigma \ D \ M \ k_2 \ d_2]^T$  (parameters appearing linearly) the state equations are described below:

$$\begin{aligned} z_1^{k+1} &= z_1^k + T z_2^k, \\ z_2^{k+1} &= z_2^k + T z_3^k, \\ z_3^{k+1} &= z_3^k - \frac{(z_4^k + z_3^k z_5^k)T}{z_6^k} + \frac{\dot{F}(k)T}{z_6^k}, \\ z_4^{k+1} &= z_4^k + 3z_2^k z_4^k z_7^k T, \\ z_5^{k+1} &= z_5^k + 18z_2^k z_3^k z_8^k T, \\ z_6^{k+1} &= z_6^k, \quad z_7^{k+1} = z_7^k, \quad z_8^{k+1} = z_8^k, \end{aligned} \quad (17)$$

where,  $T$  is the sampling time. Above state equations are used in the EKF implementation with input as force rate and measurement as the elongation/deflection of the transmission. The whole EKF procedure is omitted here for limitation in space, but it is similar to any regular EKF implementation.

## VI. MODELING THE SENSOR NOISE

The impedance estimation procedure exploiting the linearity between stiffness and elastic force, requires the knowledge of force rate in the input. The force rate is obtained using a first order filter. Fig. 7 shows a time varying force and its rate used as input to the EKF for experimental estimation of the impedance components in this article. In the estimation process, it is required to know the variances of force sensor output (and its rate) and the nature of sensor noise.

A pre-calibrated standard force gauge of IMADA make (model *DS2-200N*) is used as reference for determining the force sensor error model and calibration. Data are logged at 100 Hz frequency for a long time in a National Instruments based data acquisition system using Labview<sup>®</sup> and data are then analysed for noise content. The *White* nature of the noise is more or less observed in the left figure of Fig. 6 (see [14]). To examine the noise pattern in force rate, experiments are carried out with ramp input and data are logged. The ramp force input is obtained by using a linear spring of constant stiffness and moving the motor at slow constant velocity. Again, nearly white nature of the noise in force rate is observed, as indicated in the right figure of Fig. 6. An error model of the position sensor (encoder) has been obtained in [15]. Encoder noise as well is found to be *White* in nature. Variances obtained from experiments are 0.017N for force sensor, 0.088N/s for force rate and 0.01mm for position, which are used to form covariance matrices in the EKF procedures.

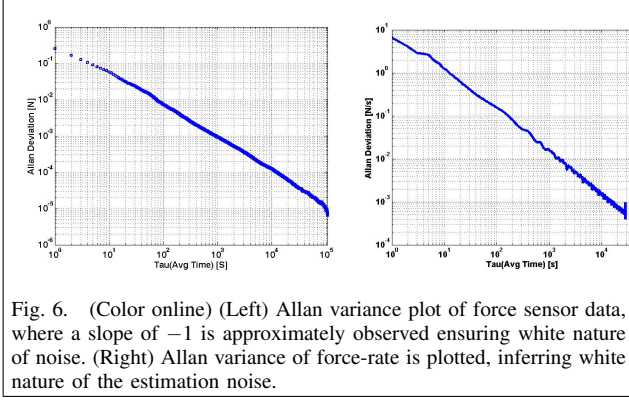


Fig. 6. (Color online) (Left) Allan variance plot of force sensor data, where a slope of  $-1$  is approximately observed ensuring white nature of noise. (Right) Allan variance of force-rate is plotted, inferring white nature of the estimation noise.

## VII. ESTIMATION RESULTS AND DISCUSSION

Extensive experiments have been carried out in estimating the impedance components of the individual transmissions as well as estimation of resulted impedance at the joint.

### A. A Least Square Static Initial Estimate

Before running the EKF, a weighted least square type parameter identification has been carried out on the elastic model of (2) through large number of experiments.

Except  $k_2$  in (2), all the unknown parameters of the elastic and damping function appear linearly in respective relationships. Therefore, this initial  $k_2$  is identified offline using a *nonlinear least square fit*. Initial identification of all other parameters are then refined by solving a over-constrained system of simultaneous equations in (18) using *Weighted Pseudo Inverse*. Defining  $X = [m \ d_0 \ d_1 \ d_2 \ k_1 \ F_0]^T \in \mathbb{R}^q$ ,  $q = 6$ ,

$$\mathcal{F} = AX + \mathcal{W}, \quad (18)$$

where  $\mathcal{F} \in \mathbb{R}^p$ ;  $\mathcal{W} \in \mathbb{R}^p$  is a zero mean disturbance vector with  $E[\mathcal{W}\mathcal{W}^T] = R_w$ ,  $A \in \mathbb{R}^{p \times q}$  have entries from logged and estimated data of position, velocity, acceleration,  $p$  being the number of logged data set. A minimum variance least square estimate,  $\hat{X}$  and its variance,  $R_X$ , can be obtained as ([16]):

$$\begin{aligned} \hat{X} &= (A^T R_w^{-1} A)^{-1} A^T R_w^{-1} \mathcal{F}, \\ R_X &= E[(\hat{X} - X)(\hat{X} - X)^T] = (A^T R_w^{-1} A)^{-1}. \end{aligned} \quad (19)$$

The *initial* elastic model identification gives the following results with variances found to be 0.0202 for  $k_1$  and 0.1741 for  $F_0$  with consistent units:

$$\begin{aligned} F_S &= 16.39 + 0.776 \exp(0.2672x), \\ F_S &= 8.269 + 7.031 \exp(0.1656x). \end{aligned} \quad (20)$$

It is found that one of the exponential-spring follows better the design characteristic in (4) than the second one. The linear springs used in the assemblies are obtained from market and they are found to deviate from the design

TABLE I. COEFFICIENTS  $k_2$ ,  $d_2$  AND  $m$  AT CONVERGENCE OF EKF ESTIMATION (WITH CONSISTENT UNITS).

At conv.	Transmission-1			Transmission-2		
	$k_2$	$d_2$	$m$	$k_2$	$d_2$	$m$
Mean	0.2711	-0.1089	0.3755	0.1673	-0.1170	0.2295
Variance $\times 10^{-4}$	0.7638	0.9851	1.053	0.8743	0.6098	0.7124

stiffness of 5N/mm. Secondly, due to small after-assembly-differences (and manufacturing tolerances), the initial force offset in the second nonlinear-spring is found to be different from the first one. The values obtained above is only for reference (to use in the initialization of the EKF). However, both the nonlinear-springs show exponential behaviour. The impedance estimation through EKF does not require the full model of the transmission, rather only a partial knowledge, which exploits the affine relation between stiffness and elastic force.

### B. Estimation through EKF procedure for individual Transmissions

The EKF formulation needs force rate as input. With a sinusoidally varying position of the motor, force input is measured by the force sensor and the force rate is estimated using a first order filter. The varying force input and force rate are reported in top two figures of Fig. 7 for one of the transmissions. Good convergence is obtained in the estimation of the states; results for one of the transmissions are shown in the bottom three figures of Fig. 7.

The results of estimation of *Generalized Stiffness*, the *Generalized Damping Rate* and *Generalized Inertia* of one of the nonlinear-transmission are presented in Fig. 8 and good convergence is observed in general. Estimation of stiffness requires only the evaluation of  $k_2$ ; similarly, estimation of damping requires only the knowledge of  $d_2$ . Values of  $k_2$ ,  $d_2$  and  $m$  at convergence are shown in Table I.  $d_2$  assumes a negative value, which is expected from the nature of the damper characteristic indicated in manufacturer's data sheet. Evolution of stiffness and damping (mean values) are illustrated in Fig. 9. However, the estimated generalized inertia (perceived dynamic mass) is found to be small; a possible reason may be that the mechanism is operated at slow speed, giving rise to very small inertial force.

### C. Joint Impedance Estimation

As described in section IV-B, once the impedance components of the individual transmissions are estimated, it becomes straightforward to find the impedance at the robot joint using the relations in (11), (12) and (13). It is to be noted that both transmission-forces and transmission-deflections are absolute. Again, since the elastic elements in the transmissions are not identical, equal position (antagonistic) inputs to the position controlled motors will cause the equilibrium position of the robot-joint to move.

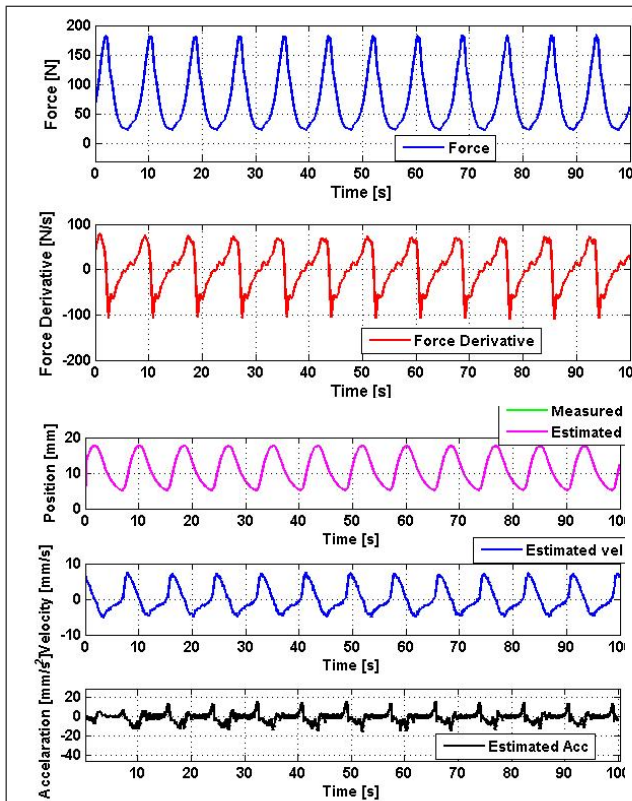


Fig. 7. (Color online) Force and force rate input to one of the nonlinear transmissions and measurements. (Top) Input force sensor reading. (Second) Estimated force rate. (Third) Measured and estimated position, (Fourth) estimated velocity, and (Fifth) estimated acceleration of deflection of the transmission.

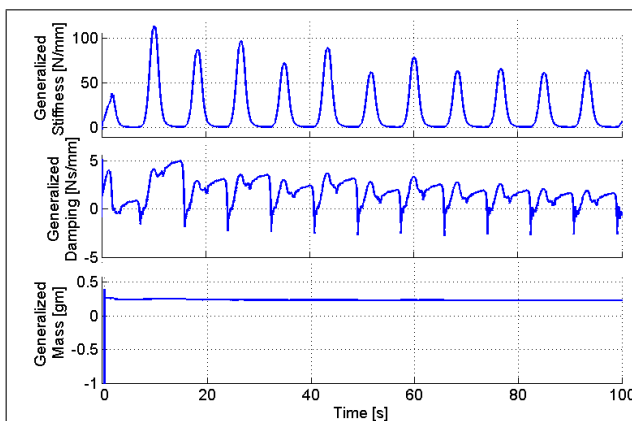


Fig. 8. (Color online) EKF procedure is formulated exploiting the stiffness-force affine relation. Results for one of the transmission are shown (mean values). (Top) Generalized stiffness. (Middle) Generalized damping. (Bottom) Generalized mass.

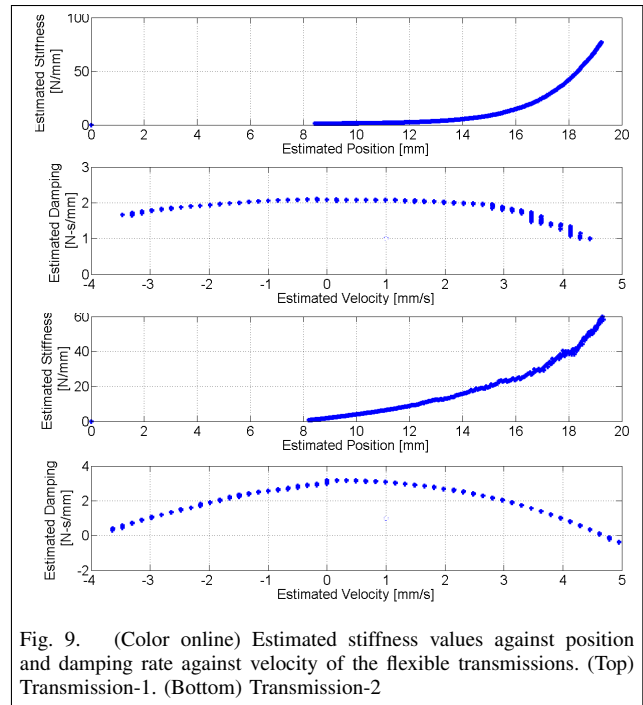


Fig. 9. (Color online) Estimated stiffness values against position and damping rate against velocity of the flexible transmissions. (Top) Transmission-1. (Bottom) Transmission-2

Experimental validation of estimation of joint impedance is beyond the scope of this article, since it will require elaborate experimental setup to apply time varying external torque input to the joint shaft. By knowing the time varying joint deflection (kept within a small value to be considered in linear range) and its rate caused by the external torque, it is possible to estimate the joint impedance about a set operating point. It is kept as future work.

It is further to be noted that *stiffness* is an intrinsic property of a flexible system. The *input dependent* stiffness in an antagonistic flexible system is a property which lies in the *null-space* of the antagonistic forces (this does not include stiffness change due to external load). In other words, input dependent stiffness is related to the *internal force* components of the antagonistic system. The tendon-force-sensor readings can be decomposed into a force component causing the motion of the joint (no external torque) and an internal force. Again, using the stiffness-force linearity of an exponential elastic function, the stiffness of the transmission and in turn the joint can readily be estimated.

## VIII. CONCLUSION

This article presents design and development of a Variable Impedance Actuator for use with robots and other machines requiring variability in actuation impedance and meant for physical interactions with operator and environment. The variability in stiffness (and impedance) is achieved passively. A passively varying stiffness (and impedance) element requires a nonlinear force-displacement elastic (and force-velocity damping) characteristic. This article presents design of such a nonlinear elastic element,

inspired by the passive characteristic of animal muscle fibre, which comes out to be an exponential one. The exponential behaviour imparts an interesting property, where, the stiffness of the element becomes linearly related with the elastic force. Development of a nonlinear damped elastic transmission is depicted in this article, starting from a biological first principle. This realization utilizes a cam and spring-loaded cam-follower mechanism, where, the cam surface is synthesized using the principle of virtual work and thus the design attains a specified desired characteristic of the transmission. Variability in damping is attained by use of a nonlinear damper obtained off-the-shelf. Among different possible realizations of variable stiffness/impedance actuation systems, this article chooses a simple antagonistic arrangement for simultaneous control of motion and stiffness variation. Subsequently, the article presents a first order Extended Kalman Filter based procedure for estimating the transmission impedances and in turn the joint impedance. The procedure advantageously exploits the property of stiffness-force linearity in the elastic system, which does not require full knowledge of the elastic function; thereby it reduces the complexity of the estimation procedure drastically, compared to the estimation using full transmission model. This reduces the uncertainties due to unmodeled parameters. The implemented Kalman procedure requires force and force rate as input and position (transmission deflection) as measurement. Noise models for force and force rate are obtained through extensive experiments and they (and that of encoder) are found to be practically white in nature to qualify for use in EKF formulation. Good tracking convergence is obtained in each of the state estimations as well as impedance component estimations. However, like any other EKF method, this procedure suffers from indeterminacy of accuracy, but achieves good repeatability. Once, the impedance components of the individual transmissions are estimated, it is straightforward to obtain the joint stiffness and impedance, where, effective tendon stiffness is also incorporated.

It is kept as future work to carry out experiments to validate the estimated joint impedance, which requires elaborate experimental setup.

#### ACKNOWLEDGMENT

The work has been done within the activities of the Institute Project OLP-152312 in CSIR-Central Mechanical Engineering Research Institute, Durgapur, INDIA.

#### REFERENCES

- [1] A. Bicchi, and G. Tonietti, "Fast and Soft Arm Tactics: Dealing with the Safety-Performance Tradeoff in Robot Arms Design and Control," *IEEE Rob. and Aut. Mag.*, vol.11, no.2, Special issue on "Safety Among Us", June, 2004.
- [2] N. Hogan, "Impedance control: an approach to manipulation, parts i, ii, iii," *Trans. of ASME, Journal of Dynamics, Systems, Measurement and Control*, Vol. 107, 1985.
- [3] H. Hanafusa, and H. Asada, "A Robotic Hand with Elastic Fingers and Its Application to Assembly Processes," in *IFAC Symposium on Information Control Problems in Production Engineering*, October, 1977, pp.127-138.
- [4] E. Burdet, R. Osu, D. Franklin, T. Milner, and M. Kawato, "The central nervous system stabilizes unstable dynamics by learning optimal impedance," *Nature*, Vol.414, No.6862, pp.446-449, 2001.
- [5] R. Schiavi, G. Grioli, Soumen Sen, and A. Bicchi, "Vsa-II: a novel prototype of variable stiffness actuator for safe and performing robots interacting with human," in *IEEE Int. Conf. on Rob. and Aut.*, Pasadena, 2008.
- [6] R. Van Ham, T.G. Sugar, B. Vanderborght, K.W. Hollander and D. Lefeber, "Compliant Actuator Designs: Review of Actuators with Passive Compliance/Controllable Stiffness for Robotic Application," *IEEE Rob. and Aut. Mag.*, vol.16, no.3, Sept. 2009.
- [7] S. Wolf, and G. Hirzinger, "A new variable stiffness design: Matching requirements of the next robot generation," in *IEEE Int. Conf. on Rob. and Aut.*, Pasadena, 2008.
- [8] A. Jafari, N Tsagarakis, B. Vanderborght and D. Caldwell, "A novel actuator with adjustable stiffness (AwAS)," in *Proc. IEEE/RSJ Int. Conf. on Intelligent Robots and systems*, pp. 4201-4206, 2010.
- [9] J. Pinto and Y. Fung, "Mechanical properties of the heart muscle in the passive state," *Journal of Biomechanics*, vol. 6, 1973.
- [10] Soumen Sen and Antonio Bicchi, "A Nonlinear Elastic Transmission for Variable-Stiffness-Actuation: Objective and Design," in *Proc. 15<sup>th</sup> National Conf. on Machine and Mechanisms*, Chennai, Nov.29-Dec.01, 2011.
- [11] Roberto Filippini, Soumen Sen, Antonio Bicchi, "Toward Soft Robots You Can Depend On: A Study of Antagonistic Actuation," *IEEE Robotics and Automation Society Magazine*, Special issue on "Adaptable Compliance, design, control, and applications of robotic stiffness actuators," Vol.15, No.3, September, 2008, pp.31-41.
- [12] G. Grioli and A. Bicchi, "A Non-Invasive, Real-Time Method for Measuring Variable Stiffness," in *Proc. Robotics Science and Systems (RSS 2010)*, Zaragoza, E, June 2010.
- [13] F. Flacco and A. De Luca, "Residual-based stiffness estimation in robots with flexible transmissions," in *Proc. IEEE Int. Conf. on Robotics and Automation*, Shanghai, May, 2011.
- [14] N. El-Sheimy, H. Hou, and X. Niu, "Analysis and Modeling of Inertial Sensors Using Allan Variance," *IEEE Tran. on Instrumentation and Measurement*, Vol.57, No.1, Jan., 2008.
- [15] S. Jain, S. Nandy, G. Chakraborty, C. S. Kumar, R. Ray and S. N. Shome, "Error Modeling of various sensors for Robotics application using Allan Variance Technique," in *Proc. IEEE Int. Conf. on Signal Processing, Communications, and Computing (ICSPCC-2011)*, Xian, China, Sep. 2011.
- [16] R. Plackett, "Some theorems in least squares," *Biometrika* 37 (1-2), pp. 149-157, 1950.